Hindawi Publishing Corporation
Smart Materials Research
Volume 2013, Article ID 932568, 10 pages
http://dx.doi.org/10.1155/2013/932568

Research Article

Nondestructive Wireless Monitoring of Early-Age Concrete Strength Gain Using an Innovative Electromechanical Impedance Sensing System

C. P. Providakis, E. V. Liarakos, and E. Kampianakis

Applied Mechanics Lab, Department of Applied Sciences, Technical University of Crete, 73100 Chania, Greece

Correspondence should be addressed to C. P. Providakis; cpprov@mred.tuc.gr

Received 1 March 2013; Accepted 22 March 2013

Academic Editor: Kong Ling Bing

Monitoring the concrete early-age strength gain at any arbitrary time from a few minutes to a few hours after mixing is crucial for operations such as removal of frameworks, prestress, or cracking control. This paper presents the development and evaluation of a potential active wireless USB sensing tool that consists of a miniaturized electromechanical impedance measuring chip and a reusable piezoelectric transducer appropriately installed in a Teflon-based enclosure to monitor the concrete strength development at early ages and initial hydration states. In this study, the changes of the measured electromechanical impedance signatures as obtained by using the proposed sensing system during the whole early-age concrete hydration process are experimentally investigated. It is found that the proposed electromechanical impedance (EMI) sensing system associated with a properly defined statistical index which evaluates the rate of concrete strength development is very sensitive to the strength gain of concrete structures from their earliest stages.

1. Introduction

Since accurate field measurements of early-age concrete properties, such as setting time, in-place strength gain, and shrinkage stresses, are crucial to in situ quality control of concrete, various techniques have been proposed including Windsor and pullout probe tests, ultrasonic pulse velocity, impact-echo method, microwave method, and maturity method [1]. Those nondestructive techniques interactively measure certain mechanical properties of the concrete from which information on the strength is derived. However, although mechanical wave velocity methods such as the ultrasonic pulse velocity and impact-echo methods are widely used to test in a nondestructive manner, they have some limitations that restrict practical applications. Thus, mainly due to their serious drawbacks they received little interest from the construction community. Besides, these methods use extensive wiring systems to operate and necessitate special equipment to gain access to the structure during construction. In addition, these techniques perform localized measurements, and the monitoring of large concrete structures requires an extensive amount of time and effort leading to costly usage. Substructures such as concrete foundations and piles are inaccessible and their early-age strength development cannot be evaluated using these monitoring systems.

The advent of smart materials, such as piezoelectric materials, shape-memory alloys, and optical fibers, has attracted interests among researchers and engineers to develop new nondestructive monitoring techniques. The key advantage of using these materials as sensing devices is that they can be placed anywhere even in remote and inaccessible locations to monitor concrete structures. In particular, the electromechanical impedance (EMI) sensing technique which employs piezoelectric transducers has been successfully emerged as a very promising technique for the strength development monitoring of concrete at early-age conditions in the works of Tawie and Lee [2], Shin et al. [3], and Shin and Oh [4]. They showed that the electromechanical impedance monitoring technique utilizing high frequencies in the range of 30–400 kHz to electrically excite the PZT-impedance transducers

bonded on the surface of the host structure by means of alternating electrical field source can monitor the changes in the mechanical impedance signatures of the tested structures. Those changes on the impedance over time based on statistics metrics like root mean square deviation (RMSD), mean absolute percentage deviation (MAPD), and correlation coefficient deviation (CCD) were shown to be an indicator of the hardening of concrete during curing process. However, findings from these studies show that they could not monitor the early hydration of fresh concrete occurring in the first three days since concrete needed to be hardened, followed by surface drying and one more day for hardening of the epoxy. An extension of the surface bonded PZT sensing technique was the introduction of embedded PZT transducers inside the mass of concrete as smart aggregates [5, 6].

The feasibility of reused PZT transducer setups was first investigated by Yang et al. [7, 8] using a piece of PZT bonded to a piece of aluminum or plastic enclosure with two bolts tightened inside some holes drilled in the enclosure. They acquired the PZT admittance signatures obtained from concrete specimens at different stages of the first 48 hours after casting. Their results showed that the developed reusable PZT setup in combination with RMSD indices was able to effectively monitor the initial hydration of concrete and its structural health condition. Despite the useful contribution of this work to the specific researching field, as the authors concluded their proposed monitoring system suffers from some essential weaknesses.

In the present paper, the objective was to extend the study of Yang et al. to develop an innovative reusable PZT transducer enclosed to a Teflon-based interface being strong enough to easily detach from the hardened concrete structure without any damage to the PZT or the Teflon-based enclosure while on the other hand being sensitive enough for strength development monitoring capabilities even in the first hours from concrete casting. Furthermore, in comparison with the one proposed by Yang et al. [7, 8], this reusable PZT transducer presents a more efficient design of its mounting system since: (a) it allows the decrease of the amount of epoxy resin used for the bonding of PZT patch to the Teflon-based casing which, in turn, results in the decrease of mechanical losses generated from epoxy resin layer's damping effect, and (b) it provides adequate waterproofing to the PZT transducer. This specially designed Teflon-based enclosure was firstly proposed in a previous work of the present authors [9]. Here, the development of this sensing system is further optimized in order to overcome some limitations of its first application.

Conventionally, the EMI measuring method required the use of bulky, expensive, and not suited for permanent placement impedance analyzers. Recently, Analog Devices Inc. [10] has made available an impedance converter network analyzer, termed as AD5933, a new system-on-chip miniaturized and fully integrated electrical impedance spectrometer, which might allow the implementation of minimum-size instrumentation for electrical impedance measurements. In the study of Park and Kim [11], a series of efforts were presented to confirm the applicability of the EMI technique using both wired and wireless sensing systems based on AD5933 chip for monitoring on the strength development during the curing process of concrete. But, although they extended the previous researches for multifunctional and environment-friendly uses in the impedance-based structural health monitoring (SHM) process, the main drawback of this work was that their first impedance measurement should be carried out 3 days after concrete mixing because before 3 days, the piezoelectric sensors could not be attached completely to the fresh concrete surface, since concrete behaves almost like a liquid at its very early stages. In the present work, the core of the measurement system is the evaluation board for the AD5933 circuit provided by Analog Devices, the EVAL-AD5933EB.

The adoption of wireless technology in structure health monitoring eliminates the need to install cable for data communication. This is especially beneficial in large-scale structures. The application of the impedance method to large-scale complex structures demands the deployment of a dense array of sensors up to hundreds and thousands in quantity. This increase in sensor numbers potentially produces difficulties and complexities in data acquisition and processing. Therefore, the integration of wireless telemetry systems into the impedance-measuring unit is imperative to manage and operate the sensing devices. Tests of wireless impedance-based monitoring systems on real structures have already been conducted in previous studies [12–14] to compare their performance on measuring electromechanical impedance variations with that of a cable-based monitoring system.

The focus of this paper is to introduce a cost-effective, reusable, and reliable nondestructive monitoring device using PZT patches enclosed in appropriate Teflon-based cases for early-age monitoring of concrete structures. This innovative sensing device is extremely cheap and is interrogated wirelessly using wireless USB connectivity to remotely measure electromechanical impedance changes on the PZT surface. The core of the proposed miniaturized sensing system is the evaluation board of AD5933 chip. Preliminary experimental data for proof of concept is presented here. This innovative PZT transducer was termed firstly in [9] as wireless Teflon-based integrated monitoring system or rather T-WiEYE.

2. Principle of Electromechanical Impedance-Based Concrete Strength Development Monitoring Using PZT Patches

Generally, electromechanical impedance- (EMI-) based SHM techniques utilize small PZT patches attached to a host structure as self-sensing actuators to excite the structure with high-frequency excitations and monitor the changes in the electrical impedance of the patch. The self-sensing properties of the PZT allow one piece of material to sense the input voltage and measure the output current. Since the PZT is bonded directly to the structure of interest, it has been found that the mechanical impedance of the structure is directly correlated with the electrical impedance of the PZT. The basis of EMI sensing technology is the energy transfer between PZT and host structure. If the PZT attached on the structure

is driven with a sinusoidal voltage, it causes the local area of the structure to vibrate (the converse piezoelectric effect) while the structural response causes an electrical response on the PZT surface (the direct piezoelectric effect). By observing some changes of the EMI signatures measured at the PZT, assessments can be made about the structural condition and integrity of the host structure. Liang et al. [15] first proposed a one-dimensional analytical model taking into account a transversally isotropic and elastic piezoelectric material and showed that the electrical impedance function, $Z(\omega)$, which represents the inverse value of electrical admittance function, $Y(\omega)$, at a given angular frequency ω is directly correlated to the local mechanical impedance of the host structure and as a complex number; it consists of a real part and an imaginary part as shown in the following equation:

$$\begin{aligned} Z(\omega) &= \frac{1}{Y(\omega)} = R + iX \\ &= -i\frac{h}{\omega w l}\left(Z_a + Z_{\text{st}}\right) \times \left(Z_a \left\{ d_{31}^2 \overline{Y}_p^E \left(\frac{\tan(kl)}{kl} - 1 \right) + \bar{\varepsilon}_{33} \right\} \right. \\ &\qquad \left. + Z_{\text{st}} \left(\bar{\varepsilon}_{33} - d_{31}^2 \overline{Y}_p^E \right) \right)^{-1}, \end{aligned} \tag{1}$$

where $i = \sqrt{(-1)}$, R and X are the impedance real and imaginary parts respectively, w, l, and h PZT plane transducer depth, length and width, respectively, $\bar{\varepsilon}_{33} = \varepsilon_{33}\varepsilon_0(1 - i\delta)$ the complex relative electrical permittivity consisting of relative permittivity ε_{33} of PZT, $\varepsilon_0 = 8.854e - 12$ ($C^2/N/m^2$) vacuum electrical permittivity and δ PZT dielectric loss factor, d_{31} (C/N) the PZT piezoelectric coefficient, $\overline{Y}_p^E = Y_p^E(1 + in)$ the complex Young's Modulus of PZT consisting of Young's Modulus Y_p^E along the transducer vibration plane and mechanical loss factor n, Z_a PZT patch mechanical impedance, Z_{st} host structure mechanical impedance, and k the angular wave number of transmitting wave to piezoelectric material interior. Transducer mechanical impedance is obtained by using the following equation [15]:

$$Z_a(\omega) = \frac{wh\overline{Y}_p^E k}{i\omega \tan(kl)} = \frac{\overline{K}_a}{i\omega}\frac{kl}{\tan(kl)}, \tag{2}$$

where $\overline{K}_a = wh\overline{Y}_p^E l^{-1}$ is the complex mechanical stiffness of PZT patch in direction of transducer's vibration. It could be stated that the host structure mechanical impedance behaves in a similar way with that described for PZT mechanical impedance through (2) yielding a strong relation with host structure structural stiffness and mechanical properties too. Generally speaking, structural impedance Z_{st} would contain both a term which depicts the host structure's material stiffness and a trigonometric function of wave number which corresponds to the transmitting wave at host structure's material interior. Any changes to host structure integrity or stiffness around the neighborhood of transducer's placement area would directly affect structural impedance amplitude because of stiffness alteration while in the same time structural impedance signature peaks shift as a function of frequency.

Moreover (1) defines that the attachment of PZT patch to the structure couples the mechanical impedance of the structure to the electrical impedance. If the mechanical property of the PZT patch does not change over the monitoring period, then the electrical impedance of the PZT-structure interaction system (Z in (1)) is solely dependent on the mechanical impedance of the host structure (Z_{st}). Any change of the mechanical properties in a structure causes changes in the mechanical impedance and also induces changes in the electrical impedance of the PZT patch bonded to the structure. In this study, this coupling property (between the electrical and mechanical impedance) of the PZT patch is utilized for strength gain monitoring, which enables one to measure the impedance changes (and hence strength changes) in concrete during curing.

3. Experimental Implementation

3.1. T-WiEYE Sensor Design. We decided to use for our piezoelectric material lead zirconate titanate (PZT). For this work, we use a PZT patch of type PIC151 with a size of $10 \times 10 \times 0.2$ mm produced by PI Ceramic Co. [16]. The packaging of the proposed T-WiEYE sensor was a major consideration since it must perform multiple functions: (a) provide an appropriate solid mounting interface between PZT material and host structure especially in the case of fresh concrete stages during the first hours from mixing (e.g., to ensure that stress waves generated can be transmitted with minimal power loss) when the concrete behaves almost as a liquid-type material with very low stiffness, (b) guarantee power and data connections to and from PZT materials, (c) protect PZT materials from natural, mechanical, and electrical environments, including temperature, moisture, strain, and impact, and finally (d) avoid durability issues for PZT materials, fatigue and creep. To meet these requirements, we chose to use a properly designed Teflon casing (Figure 1) as an enclosure of the piezoelectric patch since it has the additional ability to withstand except the above-mentioned some extra difficulties in the packaging of the T-WiEYE sensor because of the harsh environment created by fresh concrete (pH of 14). Furthermore, with the use of Teflon as enclosure material we achieved to overcome the problem observed in the reusable sensor proposed in the works of Yang et al. [7, 8] where some cement hydration residues had the tendency to stick and be remained on the surfaces of their proposed sensors, and thus, the repeatability of their measures has been slightly affected after a few reuses. A two-component adhesive, Henkel's Rapid Loctite Epoxy has been used to bond the PZT patch to the Teflon casing. Since the Teflon-based enclosure needs to be strong enough to withstand early-age concrete microstrains and any incidental impact action, the designed dimensions were 52 mm in diameter and 25 mm in depth.

Two 1/8″ diameter holes were drilled through the outer perimetrical wall of the Teflon-based enclosure and a custom-made circular plate was also fabricated from the same Teflon material and finally placed as the cap of the enclosure. This

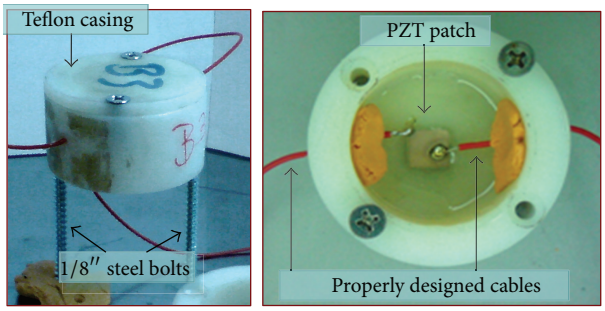

Figure 1: T-WiEYE setup.

cap design allows for more flexibility due to its impact resistance and moisture sealing property of Teflon material while on the other hand this specific cap design gave a removable top of the sensor for any future integration and repair activity. The idea was integrated by the use of two 1/8″ diameter steel bolts tightened inside the drilled holes to ensure a solid mounting of the cap to the sensor perimetrical wall and simultaneously of the whole T-WiEYE sensor package to the surface of fresh concrete. The PZT patch was soldered to a shielded cable that was connected on the other end to one of the pin connectors located on the evaluation board EVAL-AD5933 of AD5933 impedance miniaturized chip. To insert the cables with the PZT patch on the end, two small notches were cut in the side of the Teflon perimetrical wall of T-WiEYE sensor. Later, these notches were sealed with a Dow corning RTV 3140 coating silicon elastomer film [17] for waterproofing reasons.

3.2. AD5933 Impedance Miniaturized Chip. The main component of the proposed measurement system is the miniaturized impedance network converter integrated circuit AD5933 provided by Analog Devices Inc. [10]. The impedance measurement system by itself is the evaluation board EVAL-AD5933 of the AD5933 circuit which was developed by Analog Devices Inc. for demonstration purposes. Using a USB connection and provided software, a user can make impedance measurements in the range of 10–100 kHz. According to Analog Devices developers guide and demonstrated implementations of AD5933 board, the accuracy of the specific system is restricted within this frequency range (10–100 kHz) because of serious inaccuracies especially at the domain of the phase measurement for sweeping frequencies under 10 kHz and over 100 kHz [10]. The AD5933 primarily records the magnitude of the impedance. However, phase is also recorded, and the real and imaginary impedance components can be saved.

The AD5933 circuit permits the user to perform a frequency sweep with a user-defined start frequency, frequency resolution, and number of points in the sweep. In addition, the device allows the user to program the peak-to-peak value of the output sinusoidal signal as an excitation to the external unknown impedance connected between the VOUT and VIN pins (Figure 2). The excitation signal is then passed through a programmable gain stage and output into the device of

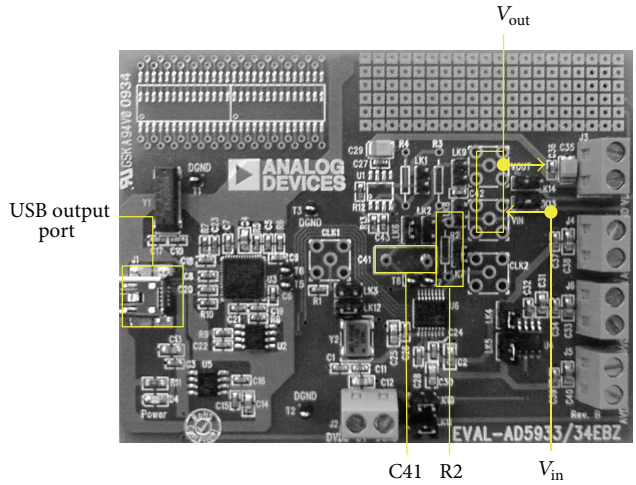

Figure 2: Functional diagram of AD5933 evaluation board. (Analog Devices, USA: http://www.analog.com/).

interest. The current output from the device due to the excitation signal is then passed through a current-to-voltage amplifier, which features a user-selectable feedback resistor (R2 part in Figure 2) in order to vary the amplifier gain. The amplifier feedback resistor must be sized appropriately in order to ensure that the signal remains in the linear range of the analog-to-digital converter (ADC). The output from the current to voltage amplifier is then sent through a low-pass antialiasing filter and sent to a 12-bit, 1 MSPS ADC. A Hanning window is applied to the digital data, and a 1024-point discrete Fourier transform (DFT) is performed at the frequency point of interest. The resulting real and imaginary values of the DFT are passed to a microcontroller in two's complement format. This procedure is repeated for every point in the desired frequency sweep. Our final T-WiEYE sensor device incorporating this evaluation board would be a miniaturized intelligent impedance sensor, which records the impedance sensing data on a single chip, and wirelessly provides the status of the early-age concrete strength development of the structure to an end user.

All the documentation related to the AD5933 evaluation board, schematics, user manual, and software is also available at the Analog Devices Inc. website [10].

3.3. The Proposed Integrated Monitoring System. A functional diagram of the whole impedance-based integrated monitoring system T-WiEYE is presented in Figure 3. T-WiEYE monitoring system utilizes a piezoelectric (PZT) transducer enclosed in the Teflon-based case as described previously, an evaluation board of AD5933 impedance measurement chip, a 802.11 g wireless four-port USB 2.0 sender and receiver system of Gefen LLC [18] and a computer, as shown in Figure 4. The user can power the evaluation board EVAL-AD5933 circuitry from its USB port. In the same time, the user can interface with the AD5933 circuit through a USB microcontroller which generates the required I2C signals to communicate with AD5933 circuit. This USB microcontroller is included in EVAL-AD5933 circuitry. The Visual Basic graphic user

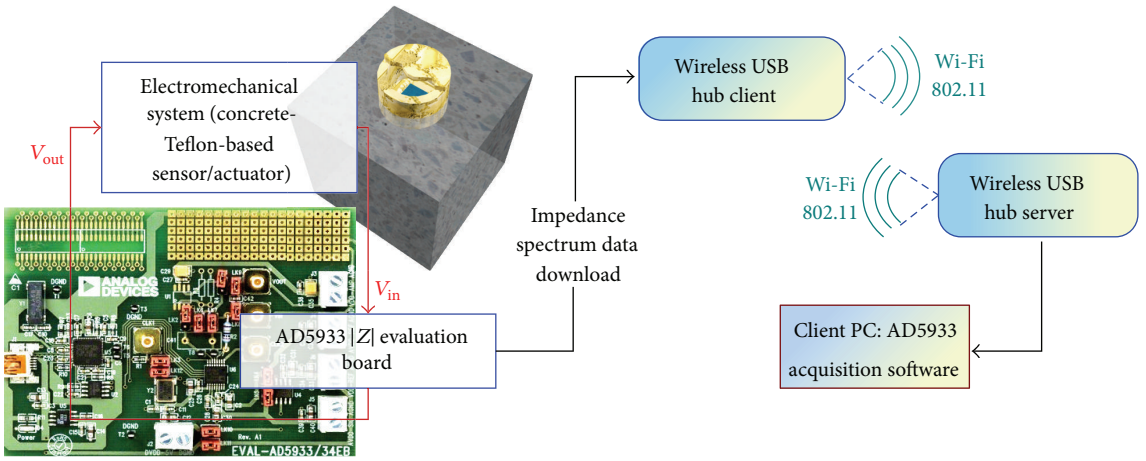

Figure 3: Functional diagram of the proposed integrated T-WiEYE monitoring system.

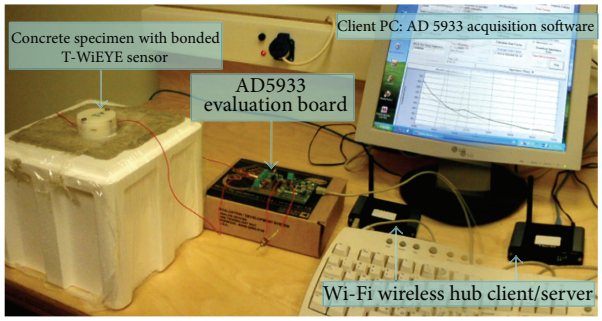

Figure 4: Laboratorial implementation of T-WiEYE concrete strength monitoring system.

interface which is provided by Analog Devices to activate the USB microcontroller is located on and run from the user PC. Using the USB interface, the microcontroller transmits the measured data providing data storage. Additionally, the microcontroller also provides an initial configuration of the integrated circuit AD5933 that is needed at the measurement beginning. In order to adapt the open-source Analog Devices' code to the present work specifications, some functionality, have been added to automatically measure the required impedance response spectrum in predefined constant time interval. After the measurement in the respective time window is done, the microcontroller reads and transmits the data from AD5933 circuit for data storing and further processing.

3.4. Wireless Telemetry System. The wireless telemetry system selected for the proposed integrated monitoring system was the 802.11 g wireless USB 2.0 Extender system of Gefen LLC. This system is composed of two separate units. The wireless USB 2.0 sender unit which provides the freedom to operate up to four USB sensors like the PZT one attached to the evaluation board EVAL-AD5933 circuit. Then, an IEEE 802.11 g radio platform is used to wirelessly communicate between the wireless USB 2.0 sender unit and the wireless USB 2.0 receiver unit using the 2.4 GHz radio frequency range. The wireless USB 2.0 sender unit and the wireless USB 2.0 receiver unit have been "paired" during manufacturing. This means that they will only communicate with each other, even if other wireless USB 2.0 units are installed nearby. The Wireless USB 2.0 Extender provides the freedom to connect high-performance and high-speed USB peripherals anywhere up to 30 meter from the CPU. In the same time, it gives instant access to data (up to 54 Mbps) with zero wires. Wireless High speed USB 2.0 transmits data up to 54 Mbps allowing for little or no downtime. The wireless sender unit is connected to the EVAL-AD5933 circuity while the wireless receiver unit is connected to the PC. The Wireless USB 2.0 Extender will automatically establish a wireless connection between the Wireless USB 2.0 Sender unit and the Wireless USB 2.0 Receiver unit once power is applied to both units and they are located within their operating range.

4. Results and Discussion

4.1. Experimental Setup. Three concrete cubic specimens, C1, C2, and C3 with dimensions of 150 × 150 × 150 mm, which is normally used for compressive strength evaluation, were prepared for this experiment comprising of type I Portland cement (C), water (W), well-graded washed sand (FA), middle-size aggregates (MA), and gravel coarse aggregate (CA). The mixing proportion of the concrete is 1.0 : 0.62 : 1.36 : 1.35 : 2.76 (C : W : FA : MA : CA, ratio by mass of cement). The concrete specimens have been allowed to cure inside a mold made of expanded polystyrene matrix to maintain almost adiabatic conditions. A PIC151 PZT patch was instrumented inside T-WiEYE sensing system by pressing with weights and protective padding until the adhesive was fully cured. T-WiEYE sensing system, in turn, was bolted by tightening it to the upper surface of fresh concrete specimen as shown in Figure 4. PZT leads were wounded and taped to the T-WiEYE wall to protect them from damage during transportation to the testing apparatus. After concrete hardening, the two bolts will be unscrewed and the PZT and enclosure will be removed for future applications. The installation of T-WiEYE system on the

surface of the fresh concrete was done 3 hours after casting of the cubic specimens when T-WiEYE system started to acquire electromechanical impedance signatures. To ensure that the signal remained in the linear range of the analog-to-digital converter, a feedback resistor is installed to a properly founded port of AD 5933 evaluation board, signed as R2 to Figure 2, equal to R2 = 220 ohms. This value of applied feedback resistor is approached by testing different resistors for the several set of impedance measurements and taking proportionally to each case impedance signatures. These signatures were evaluated by a reference signature taken from a laboratorial impedance analyzer.

The first electromechanical impedance measurement was carried out at the age of 3 hours in order to ensure full curing of PZT bonding adhesive. Then impedance signatures were acquired continuously every 3 hours for the first day, then every 12 hours for the next 6 days, and after the 7th day the acquisition was performed at the 10th, 14th, 21st, and finally at 28th days. The impedance signatures are measured at a frequency range of 50–70 kHz from the self-sensing T-WiEYE system so that, finally, they contain 200 data points. This frequency range was based on the results of previous experiments in which impedance signatures were acquired at a frequency range of 10–100 kHz. At this range, it was observed that for frequencies between 50 and 70 kHz there were the most sensitive to concrete hardening changes impedance signature features. In order to minimize incoherent noise components, the signatures were acquired with four repeated measurements and averaged.

4.2. RMSD-Based Concrete Strength Development Metric. Figure 5 shows the real and imaginary parts of the electromechanical impedance for the 3-hour measurement case and for all subsequent hours' measurement cases. In this figure, it is seen that the strength development process not only shifts in the resonant frequency of the real part of electromechanical impedance, but also changes its amplitude. It is very interesting to observe that the imaginary part of electromechanical impedance shown in Figures 5(a), 5(b), and 5(c) depicts an almost expected linear variation and, in the contrary to the results of 100–400 kHz frequency studies of Shin et al. [3], at the currently investigated lower frequency range of 50–70 kHz plays a dominant and more or less an active role and therefore should be used in the subsequent analyses. To account for the overall change in the impedance spectra during the concrete curing process, those changes can be processed using statistics metrics such as root mean square deviation (RMSD) which is commonly used in structural health monitoring of structures as damage indices. The RMSD metric is given as

$$\mathrm{RMSD}\,(\%) = \sqrt{\frac{\sum_{n=1}^{F}\left[\mathrm{Re}\left\{Z\left(\omega_n\right)\right\} - \mathrm{Re}\left\{Z_0\left(\omega_n\right)\right\}\right]^2}{\sum_{n=1}^{F}\left[\mathrm{Re}\left\{Z_0\left(\omega_n\right)\right\}\right]^2}} \times 100, \tag{3}$$

where F is the number of sample points in the impedance spectra (in the present case $F = 200$), where $Z(\omega_n)$ is the real part of impedance (resistance) of the nth frequency of a specific day and $Z_0(\omega_n)$ is the resistance of the nth frequency of the 3rd hour of the concrete curing process.

The variation of the calculated RMSD value in terms of the curing hours is shown for C1, C2, and C3 specimens of this concrete mix in Figure 6. It is evidently observed that the RMSD increases as the amount of hardening of concrete proceeds and the strength development increases. Of course, as shown in Figure 6, some RMSD values measured between 120 and 156 hours from casting for the C1 specimen failed to follow the general trend since at those times there were some technical misalignments of the C1 specimen setup. Generally, if the host structure becomes stronger, implying less vibration freedom for PZT, the peaks in signature which correspond to natural frequencies of the structure will shift to the right. This same trend maintains more or less constantly until the final 28th day (672 hours from casting).

For the purposes of the present paper, we introduce, here, the term RMSD_R as the ratio between the amount of cumulative RMSD value changes and the elapsed time from the baseline measurement stage (3 hours from concrete casting). RMSD_R index is described mathematically by the following form:

$$\begin{aligned}\mathrm{RMSD\_}R\left(t_n\right) &= \frac{\sum_{j=2}^{n}\Delta\mathrm{RMSD}_j}{\sum_{j=2}^{n}\Delta t_j} \\ &= \frac{\sum_{j=2}^{n}\left(\mathrm{RMSD}_j - \mathrm{RMSD}_{j-1}\right)}{\sum_{j=2}^{n}\left(t_j - t_{j-1}\right)},\end{aligned} \tag{4}$$

where t_n is the nth sampling time from concrete casting and $t_1 = 3$ hours. Table 1 presents the values of RMSD_R index as computed by using (4) for C2 specimen. This index basically describes the rate of change of the overall RMSD values up to the measuring time. Figure 7 depicts the variation of RMSD_R index as a function of the curing time from concrete casting. From the inspection of Figure 7(b), it can be observed that the peak of the variation of RMSD_R values is reached after 9–12 hours (respective to the investigated specimen) from casting and then it is followed by a sudden decrease in RMSD_R due, mainly, to the increased hydration rate at this concrete development stage. It is very interesting to point out here that quite similar conclusion has been also observed in the work of Divsholi and Yang [8]. This indicates that the cumulative amount of changes in EMI signatures is the same with the cumulative amount of changes in the concrete strength development at its hydration period and suggests that the RMSD_R is a reliable indicator to monitor the strength gain of early-age concrete providing important information for the quality of the concrete. However, in this case, a special relationship between the RMSD_R value and the compressive strength must be set in a future study. As shown in Figure 7(a), the RMSD_R value, after 150 hours of concrete casting, behaves almost constantly up to the 28th day and maintains a value lower than 0.25. Thus, by using the RMSD_R index one can conclude that the time of 9–12 hours from casting is of potential value for the setting time of this concrete mix.

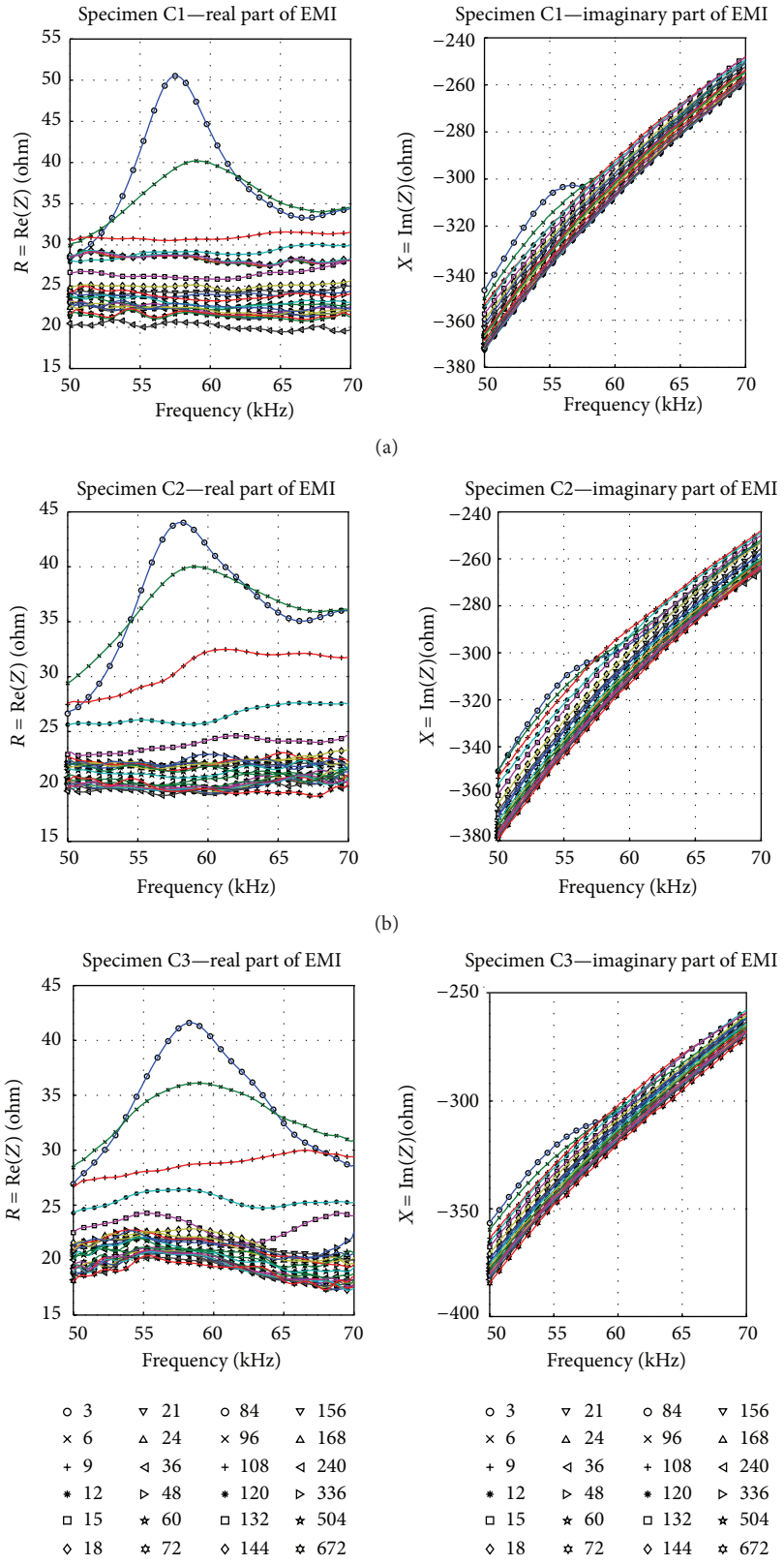

FIGURE 5: Real and imaginary parts of EMI signatures from 3 hours to 28 days (672 hours, see also figures' legends) from concrete casting: (a) C1 specimen, (b) C2 specimen, and (c) C3 specimen.

Table 1: Calculation procedure of RMSD_R index for specimen C2.

n, j	t_n (Hours)	Δt_j	$\Sigma\Delta t_j$ $j = 2 : n$	RMSD (%)	ΔRMSD_j	$\Sigma\Delta\text{RMSD}_j$ $j = 2 : n$	RMSD_R_n
1	3.00	0.00	0.00	0.00	0.00	0.00	0.00
2	6.00	3.00	3.00	5.78	5.78	5.78	1.93
3	**9.00**	3.00	6.00	19.44	13.66	19.44	**3.24**
4	**12.00**	3.00	9.00	30.42	10.98	30.42	**3.38**
5	15.00	3.00	12.00	36.77	6.35	36.77	3.06
6	18.00	3.00	15.00	40.83	4.06	40.83	2.72
7	21.00	3.00	18.00	41.61	0.78	41.61	2.31
8	24.00	3.00	21.00	41.70	0.09	41.70	1.99

Table 2: Calculation procedure of f_{cm}_R index according to Eurocode (EC2) formula (4).

n, j	t_n (Hours)	Δt_j	$\Sigma\Delta t_j$ $j = 2 : n$	f_{cm} (MPa) formula (4)	$\Delta f_{\text{cm}j}$	$\Sigma\Delta f_{\text{cm}j}$ $j = 2 : n$	f_{cm}_R_n
1	3.00	0.00	0.00	0.30	0.00	0.00	0.000
2	6.00	3.00	3.00	1.20	0.90	0.90	0.300
3	**9.00**	3.00	6.00	2.22	1.02	1.92	**0.320**
4	**12.00**	3.00	9.00	3.20	0.98	2.90	**0.323**
5	15.00	3.00	12.00	4.11	0.91	3.81	0.318
6	18.00	3.00	15.00	4.95	0.84	4.65	0.310
7	21.00	3.00	18.00	5.71	0.76	5.41	0.301
8	24.00	3.00	21.00	6.41	0.70	6.12	0.291

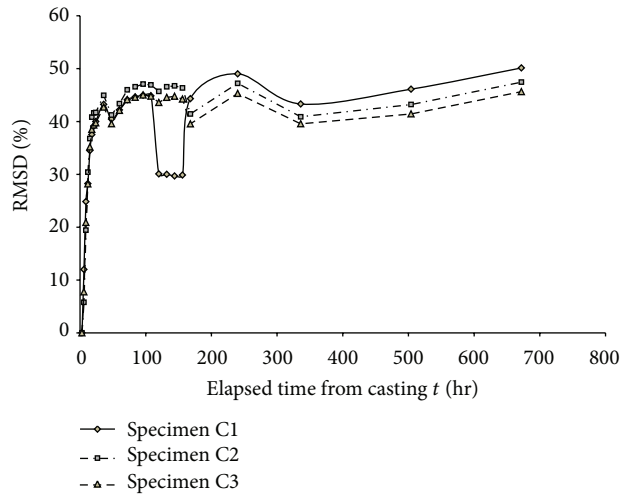

Figure 6: RMSD index variation from 3 hours to 28 days (672 hours) from concrete casting.

Taking into account Eurocode (EC2) formula (5) [19] and assuming a value of 25 MPa for compressive strength f_{cm28} which is a comparable value to the designed compressive strength of the investigated in this paper concrete mix, we could easily estimate the development of concrete strength f_{cm} as a function of time from concrete casting. Then proceeding similarly as in the above-described case of RMSD_R index, one can obtain f_{cm}_R index values as evaluated in (6). Those f_{cm}_R index values were tabulated in Table 2 and depicted in Figure 8. Surprisingly, this figure depicts exactly the same shape as that presented in Figure 7 of this paper and indicates the same curing time step where a peak value is reached (at 9–12 hours). This leads to the conclusion that the rate of cumulative changes of concrete strength according to EC2 formula as divided by the time elapsed from the baseline measurement of 3 hours could be considered as a possible criterion of concrete setting time. However, this criterion needs further study because it may change as the baseline changes:

$$f_{\text{cm}}(t) = f_{\text{cm28}} \exp\left[s\left(1 - \sqrt{\frac{672}{t}}\right)\right] \text{(MPa)}, \quad (5)$$

where $f_{\text{cm28}} = 25$ MPa is the 28 day's concrete strength, t time in hours from concrete casting, and s a parameter which depends on cement strength development duration and varies between 0.2 and 0.38. Consider

$$f_{\text{cm}}\_R(t_n) = \frac{\sum_{j=2}^{n} \Delta f_{\text{cm}j}}{\sum_{j=2}^{n} \Delta t_j} = \frac{\sum_{j=2}^{n} \left(f_{\text{cm}j} - f_{\text{cm}j-1}\right)}{\sum_{j=2}^{n} \left(t_j - t_{j-1}\right)}, \quad (6)$$

where t_n is the nth sampling time from concrete casting and $t_1 = 3$ hours.

5. Conclusions

An innovative, wireless and miniaturized EMI-based measuring system has been design and developed. This system is

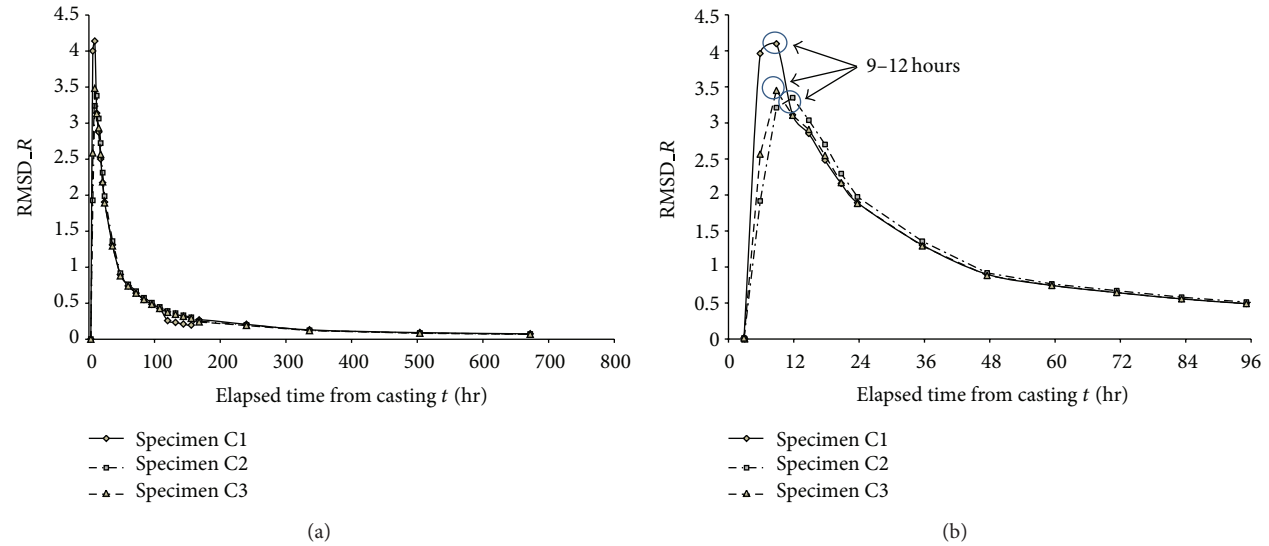

Figure 7: RMSD_*R* index variation. (a) From 3 hours to 28 days (672 hours) and (b) focus on time range between 3 hours and 4 days (96 hours).

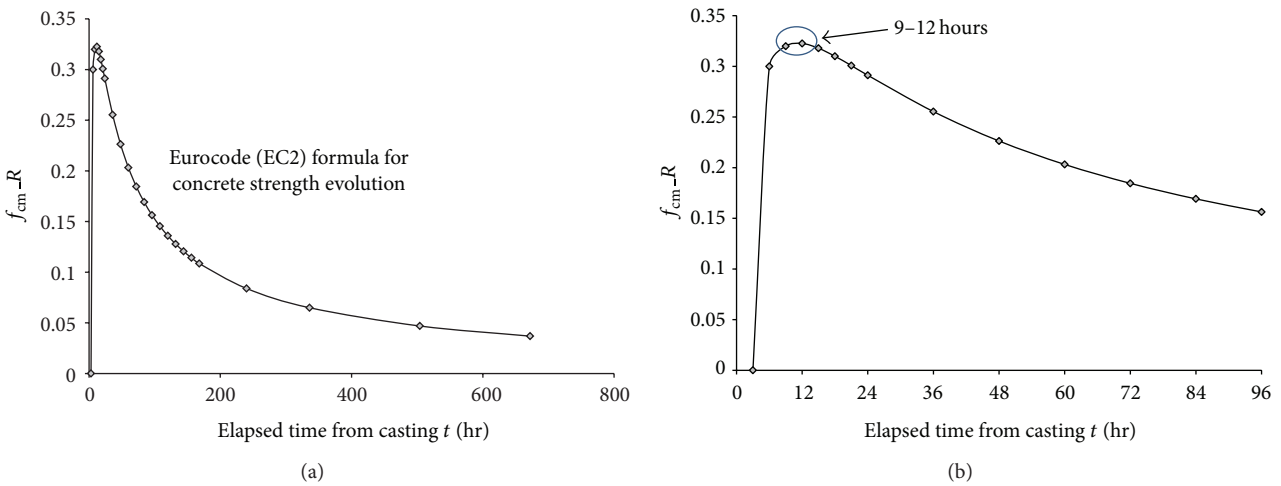

Figure 8: Cumulative value of concrete compressive strength changes according to Eurocode (EC2) formula. (a) From 3 hours to 28 days (672 hours) and (b) focus on time range between 3 hours and 4 days (96 hours).

based on a AD5933 impedance measuring chip and evaluation board installed inside a Teflon-based enclosure offering signal processing and displaying the measured EMI data through the developed software operating under Windows platform. The developed system has been designed with respect to the system portability, accuracy, and sensitivity.

Based on the experimental results, it is found that EMI signatures gradually shift to the right as the concrete curing time increases, and this verifies the applicability of the proposed EMI monitoring system. The rate of cumulative changes of RMSD as divided by the time elapsed from measurement starts indicates a peak value between 9 and 12 hours from concrete casting followed by a sudden decrease reaching an almost constant value up to the 28th day. This can be considered as a very promising tool for predicting the setting time of concrete for demolding operations.

Another advantage of the proposed EMI sensing system is that continuous monitoring can be possible with this active sensing method. In other words, once the PZT and the controlling devices are bonded on the structure, this active sensing method does not need any human intervention afterward and can acquire the signatures continuously.

Acknowledgments

This research has been cofinanced by the European Union (European Social Fund-(ESF)) and Greek National Funds through the Operational Program "Education and Lifelong Learning" of the National Strategic Reference Framework (NSRF)—Research Funding Program: Heracleitus II - Investing in knowledge society through the European Social Fund.

References

[1] ACI Committee, "In-place methods to estimate concrete strength," Tech. Rep. 228.1R-03, American Concrete Institute, Farmington Hills, Mich, USA, 2003.

[2] R. Tawie and H. K. Lee, "Piezoelectric-based non-destructive monitoring of hydration of reinforced concrete as an indicator of bond development at the steel-concrete interface," *Cement and Concrete Research*, vol. 40, no. 12, pp. 1697–1703, 2010.

[3] S. W. Shin, A. R. Qureshi, J. Y. Lee, and C. B. Yun, "Piezoelectric sensor based nondestructive active monitoring of strength gain in concrete," *Smart Materials and Structures*, vol. 17, no. 5, Article ID 055002, 2008.

[4] S. W. Shin and T. K. Oh, "Application of electro-mechanical impedance sensing technique for online monitoring of strength development in concrete using smart PZT patches," *Construction and Building Materials*, vol. 23, no. 2, pp. 1185–1188, 2009.

[5] L. Qin and Z. Li, "Monitoring of cement hydration using embedded piezoelectric transducers," *Smart Materials and Structures*, vol. 17, no. 5, Article ID 055005, 2008.

[6] G. Song, H. Gu, and Y. L. Mo, "Smart aggregates: multi-functional sensors for concrete structures—a tutorial and a review," *Smart Materials and Structures*, vol. 17, no. 3, Article ID 033001, 2008.

[7] Y. Yang, B. S. Divsholi, and C. K. Soh, "A reusable PZT transducer for monitoring initial hydration and structural health of concrete," *Sensors*, vol. 10, no. 5, pp. 5193–5208, 2010.

[8] B. S. Divsholi and Y. Yang, "Monitoring hydration of concrete with piezoelectric transducers," in *Proceedings of the 35th Conference on Our World in Concrete & Structures*, Singapore, 2010.

[9] C. P. Providakis and E. V. Liarakos, "T-WiEYE: an early-age concrete strength development monitoring and miniaturized wireless impedance sensing system," *Engineering Procedia*, vol. 10, pp. 484–489, 2011.

[10] http://www.analog.com/.

[11] S. Park and D. J. Kim, "Ubiquitous piezoelectric sensor network (USPN)-based concrete curing monitoring for u-construction," Modern telemetry, ed Ondej Krejcar In Tech, http://www.interchopen.com/books/modern-telemetry.

[12] D. L. Mascarenas, G. Park, K. M. Farinholt, M. D. Todd, and C. R. Farrar, "A low-power wireless sensing device for remote inspection of bolted joints," *Proceedings of the Institution of Mechanical Engineers, Part G: Journal of Aerospace Engineering*, vol. 223, no. 5, pp. 565–575, 2009.

[13] J. Min, S. Park, C. B. Yun, and B. Song, "Development of a low-cost multifunctional wireless impedance sensor node," *Smart Structures and Systems*, vol. 6, no. 5-6, pp. 689–709, 2010.

[14] S. Park, J. W. Kim, C. Lee, and S. K. Park, "Impedance-based wireless debonding condition monitoring of CFRP laminated concrete structures," *NDT&E International*, vol. 44, no. 2, pp. 232–238, 2011.

[15] C. Liang, F. Sun, and C. A. Rogers, "Electro-mechanical impedance modeling of active material systems," *Smart Materials and Structures*, vol. 5, no. 2, pp. 171–186, 1996.

[16] PI Ceramic GmBH, http://www.piceramic.com/.

[17] Dow Corning commercial site, http://www.dowcorning.com/.

[18] Gefen LLc commercial site, http://www.gefen.com/.

[19] P. Bamforth, D. Chisholm, J. Gibbs, and T. Harisson, "Properties of concrete for use in eurocode 2," The Concrete Center Report CCIP-029, 2008, http://www.concretecenter.com/.